

Supporting Information

Cu(I) and Cu(II) complexes based on Ionidamine-conjugated ligands designed to promote synergistic antitumor effects

Fabio Del Bello,^a Maura Pellei,^{*b} Luca Bagnarelli,^b Carlo Santini,^b Gianfabio Giorgioni,^a Alessandro Piergentili,^a Wilma Quaglia,^{*a} Chiara Battocchio,^c Giovanna Iucci,^c Irene Schiesaro,^c Carlo Meneghini,^c Iole Venditti,^c Nitya Ramanan,^d Michele De Franco,^e Paolo Sgarbossa,^f Cristina Marzano,^e and Valentina Gandin^e

^a*School of Pharmacy, Medicinal Chemistry Unit, University of Camerino, via S. Agostino 1, 62032 Camerino, Italy*

^b*School of Science and Technology, Chemistry Division, University of Camerino, via S. Agostino 1, 62032 Camerino, Italy*

^c*Department of Science, Roma Tre University, Via della Vasca Navale 79, 00146, Roma, Italy*

^d*Diamond Light Source, Harwell Science and Innovation Campus, Didcot, OX11 0DE, UK*

^e*Department of Pharmaceutical and Pharmacological Sciences, University of Padova, via Marzolo 5, 35131 Padova, Italy*

^f*Department of Industrial Engineering, University of Padova, via Marzolo 9, 35131 Padova, Italy*

EXAFS data analysis details

The experimental Cu K edge X-ray absorption spectra were treated along the standard procedures for data normalization and extraction of the structural EXAFS signal.¹ The quantitative EXAFS analysis was carried out using the atomic coordinates of the two residues as starting point for the data refinement that was carried out fitting the k^2 weighted structural signal $k^2\chi(k)$ in the k -space (without Fourier Filtering) in the 3-15 \AA^{-1} k -range. The appropriate single (SS) and multiple (MS) scattering paths were selected on the basis of their amplitude and statistical significance,¹ grouping in a single contribution those paths with similar geometry and composition. To reduce the correlation among the parameters the path multiplicity numbers were constrained to the molecular structure (see Table 2 of the manuscript). The experimental data, best fit and examples of the used paths are presented in Figure 4 of the manuscript. The differences among the spectra of the three samples (Figure 4A) can be understood in a more intuitive way looking at the FT moduli $|FT|$ (Figure 4B): the complex **10** data present a major main peak around 1.5 \AA (uncorrected for the phase shift), originating from 2 N at around 2 \AA and 2 Cl at around 2.2 \AA . In the next neighbour region the two main $|FT|$ features at around 2.5 \AA and 3.5 \AA (uncorrected for the phase shift) are ascribed, one to N(2) and C neighbours from the pyrazole rings (around 3 \AA), the other to the SS and MS paths to the C(2) atoms. These MS contributions are relevant due to the almost aligned configurations Cu-N-C(2), Cu-N(2)-C(2) and Cu-C-C(2).²

In complex **10**, R is a hydrogen atom, which is expected to provide a negligible EXAFS signal. On the contrary, the carbon atoms of CH_3 groups of complex **16** are expected to provide a sizable signal.

The distances and mean square relative displacement (MSRD) σ^2 obtained from the refinement are reported in Table 2 of the manuscript for SS contributions. In complex

10 the distances demonstrate a good agreement with the expected molecular structure: the Cu-N nearest neighbour shell is found at 1.96 Å, the Cl is at 2.23 Å from Cu. The Cu-C and Cu-N(2) shells are indistinguishable in complexes **10** and **15** and a single contribution (N = 4) was used (the very similar backscattering amplitude and phase functions of C and N make them difficult to distinguish in the analysis). The analysis of complex **16** requires an additional Cu-C^R contribution at around 1.89 Å. This finding definitively demonstrates the modification of Cu coordination geometry from roughly square planar (complex **10**) to roughly octahedral (complex **16**). This contribution is mandatory to achieve reliable fit; without it the Cu-Cl shell results unphysically short. It is possible that such additional contact originates from the CH₃ residue.

In complex **15** the Cu-N distance is slightly longer, due to the lower Cu(I) electronegativity providing a more loosely bound structure; a single contribution is used to reproduce the Cu-C and Cu-N(2) shells around 2.9 Å, but an additional contribution at around 3.3 Å is required. We likely assume that this last comes out from the C atoms of the phenyl rings linked to P (triphenylphosphine). In order to check the Cu(I) coordination number we refined the EXAFS signal using 2N+2P, 1N+2P and 2N+1P as Cu(I) nearest neighbour shells configurations. The best fit agreements were quantified looking at the weighted residual square function R_W^2 resulting the lowest ($R_W^2 = 0.080$) for 2N+2P with respect to the 1N+2P ($R_W^2 = 0.084$) and 2N+1P ($R_W^2 = 0.089$) models.

Table S1. XPS data analysis results: BE, FWHM, atomic percents and proposed assignments.

Sample	Signal	BE (eV)	FWHM (eV)	Experimental Atomic Ratios	Theoretical Atomic Ratios	Assignment
4	C1s	284.70	1.47	9.5	7.5	C-C aromatic
		286.79	1.47	7.1	3	C-N
		288.06	1.47	4.8	2.5	NHCO, C=N
		289.40	1.47	-	-	COOH impurities
		291.90	1.47	1	1	C-Cl
	O1s	532.44	2.73	1	1	C=O
	N1s	399.21	2.89	1.6	1.6	amine- or amide-like N-C
		401.11	2.89	1	1	imine-like N=C
	Cl2p	200.44	2.77	1	1	C-Cl
10	C1s	284.70	1.55	10	5.5	C-C aromatic and alifatic
		286.35	1.55	3	3	C-N
		288.12	1.55	2	2.5	NHCO, C=N
		289.63	1.55	-	-	COOH impurities
		291.24	1.55	1	1	C-Cl
	O1s	531.88	1.80			C=O
		533.27	1.80			C-O impurities
	N1s	399.70	3.49	1	1	amine- or amide-like N-C
	Cl2p	198.00	1.75	1.4	1	Cl-Cu (Cu(II) complex)
		200.09	1.75	1	1	C-Cl
Cu2p	936.62	3.24	1		Cu(II)-complex	
15	C1s	284.70	1.75	21	22.5	C-C aromatic and alifatic
		286.03	1.75	6	7.5	C-N, C-P

		288.01	1.75	1.8	1.5	NCO, C=N
		291.74	1.75	1	1	C-Cl
	N1s	399.97	2.74	1	1	amine- or amide-like N-C
	O1s	531.53	3.57	1	1	C=O
	P2p _{3/2}	131.15	2.00	1.6	2	PPh ₃
		138.00	2.00	1	1	PF ₆
	Cl2p _{3/2}	200.24	1.58	1	1	C-Cl
	Cu2p _{3/2}	932.37	2.22	1	1	Cu(I) complex
	F1s	685.88	2.23	F/P = 5.4	F/P = 6	PF ₆
16	C1s	284.70	1.62	9.5	7.5	C-C aromatic
		286.39	1.62	2.5	4.5	C-N
		288.33	1.62	1.3	1.5	NHCO, C=N
		289.69	1.62	-	-	COOH impurities
		291.15	1.62	1	1	C-Cl
	O1s	531.72	1.91			C=O
		532.98	1.91			C-O impurities
	N1s	400.60	3.46	1	1	amide- or amine-like N-C
	Cl2p	198.01	1.62	1.3	1	Cl-Cu (Cu(II) complex)
		200.13	1.62	1	1	C-Cl
	Cu2p	935.92	2.54	1		Cu(II) complex

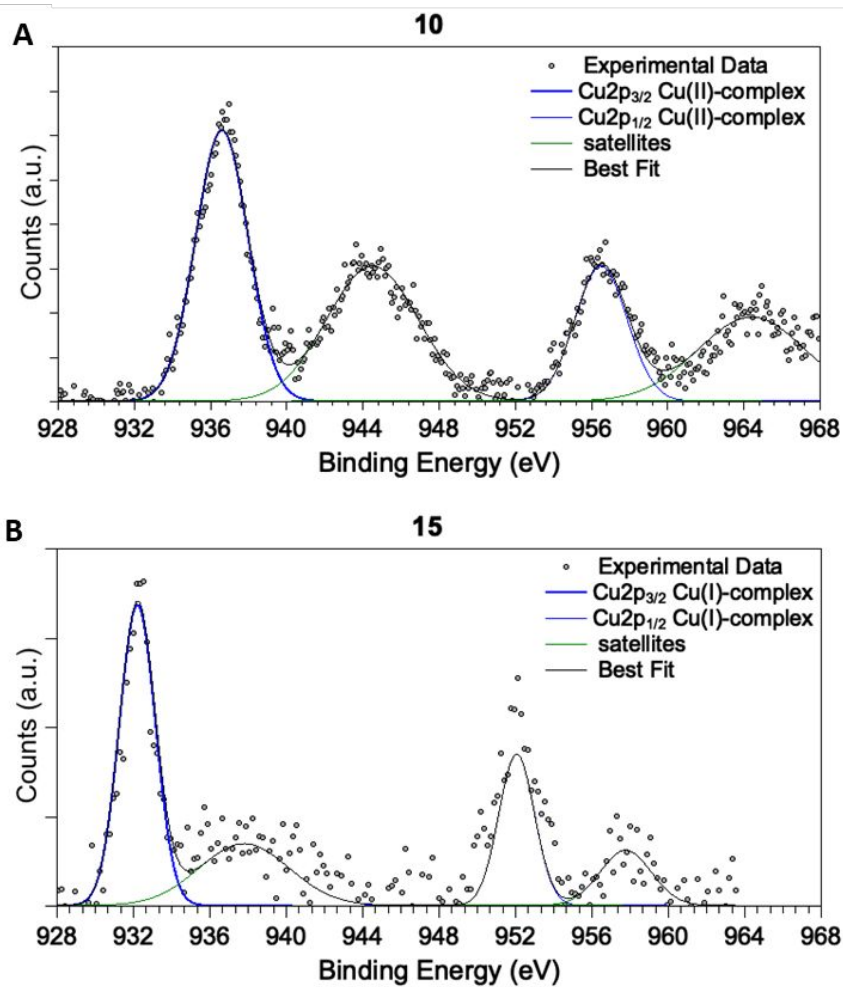


Figure S1. XPS Cu₂p spectrum of Cu(II) complex **10** (A) and Cu(I) complex **15** (B).

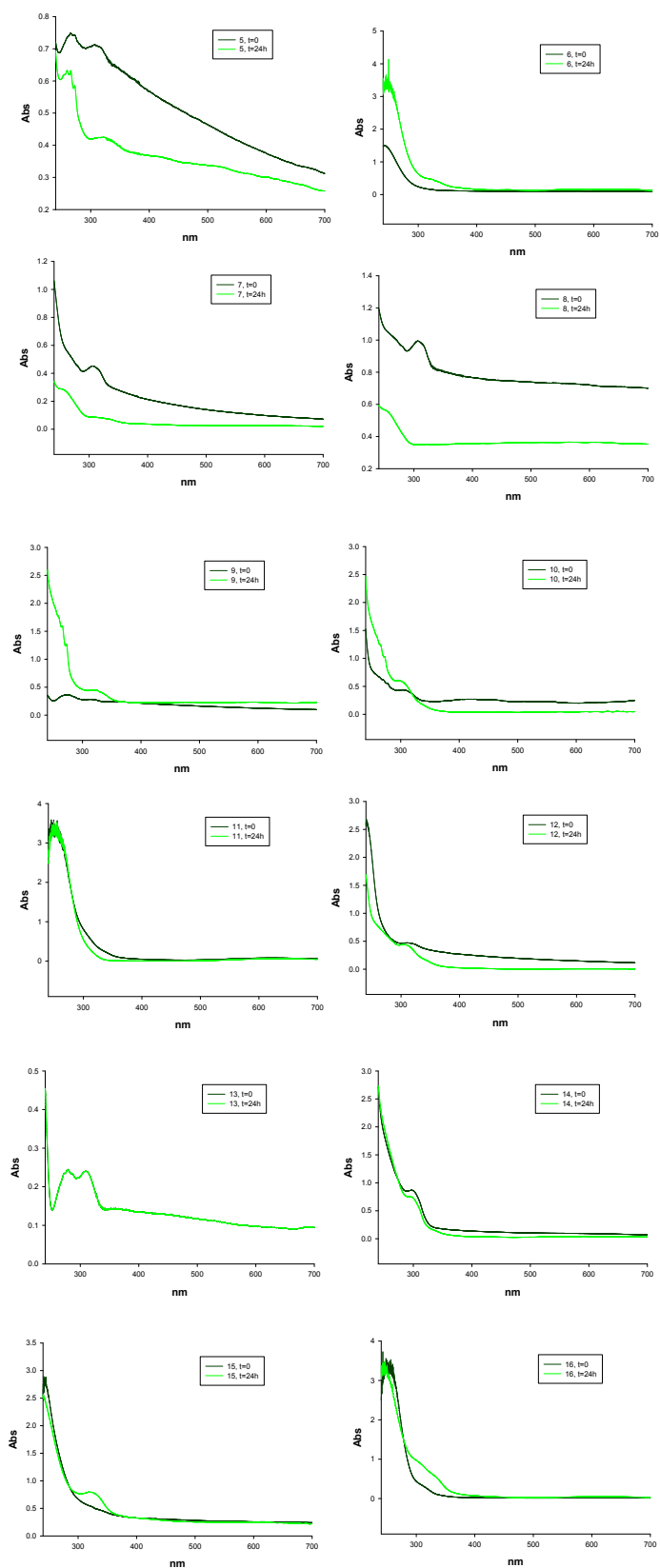


Figure S2. Stability studies. All complexes were dissolved at 50 μ M in 0.5% DMSO/RPMI. UV-visible spectra were recorded at t = 0 min and t = 1440 min = 24 h.

References

1. Meneghini, C.; Bardelli, F.; Mobilio, S. ESTRA-FitEXA: A software package for EXAFS data analysis. *Nucl. Instrum. Methods Phys. Res., Sect. B* **2012**, 285, 153-157, DOI: <https://doi.org/10.1016/j.nimb.2012.05.027>.
2. Meneghini, C.; Morante, S. The active site structure of tetanus neurotoxin resolved by multiple scattering analysis in X-ray absorption spectroscopy. *Biophys. J.* **1998**, 75 (4), 1953-1963, DOI: 10.1016/s0006-3495(98)77636-2.